Neuron, Vol. 44, 423–437, October 28, 2004, Copyright ©2004 by Cell Press

# Close Homolog of L1 Modulates Area-Specific Neuronal Positioning and Dendrite Orientation in the Cerebral Cortex

**Galina P. Demyanenko,[1] Melitta Schachner,[3] Eva Anton,[2] Ralf Schmid,[2] Guoping Feng,[4] Joshua Sanes,[5] and Patricia F. Maness[1,2,*]**
[1]Department of Biochemistry and Biophysics
[2]University of North Carolina Neuroscience Center
505 Mary Ellen Jones Building, CB#7260
University of North Carolina School of Medicine
Chapel Hill, North Carolina 27599
[3]Universitaet Hamburg
D-20246 Hamburg
Germany
[4]Department of Neurobiology
Duke University Medical School
Durham, North Carolina 27710
[5]Department of Molecular and Cellular Biology and
Center for Brain Science
Harvard University
Cambridge, Massachusetts 02138

## Summary

**We show that the neural cell recognition molecule Close Homolog of L1 (CHL1) is required for neuronal positioning and dendritic growth of pyramidal neurons in the posterior region of the developing mouse neocortex. CHL1 was expressed in pyramidal neurons in a high-caudal to low-rostral gradient within the developing cortex. Deep layer pyramidal neurons of CHL1-minus mice were shifted to lower laminar positions in the visual and somatosensory cortex and developed misoriented, often inverted apical dendrites. Impaired migration of CHL1-minus cortical neurons was suggested by strikingly slower rates of radial migration in cortical slices, failure to potentiate integrin-dependent haptotactic cell migration in vitro, and accumulation of migratory cells in the intermediate and ventricular/subventricular zones in vivo. The restriction of CHL1 expression and effects of its deletion in posterior neocortical areas suggests that CHL1 may regulate area-specific neuronal connectivity and, by extension, function in the visual and somatosensory cortex.**

## Introduction

The L1 family of cell adhesion molecules (CAMs) regulates neural functions pivotal to nervous system development, including cell adhesion, axon guidance, and synaptic plasticity (Panicker et al., 2003). The L1 family is comprised of four structurally related transmembrane proteins in vertebrates: L1, the Close Homolog of L1 (CHL1), NrCAM, and neurofascin. Each molecule consists of six immunoglobulin (Ig)-like domains, four to five fibronectin type III domains, and a conserved cytoplasmic domain that binds the actin cytoskeletal adaptor ankyrin. Their extracellular regions engage in multiple homophilic and heterophilic interactions with cell surface molecules such as integrins and immunoglobulin-class receptors, activating intracellular signaling pathways that carry out their cellular functions.

CHL1 is the most recently identified member of the L1 family. Its amino acid sequence is ~60% identical to L1 in the extracellular region and ~40% identical in the cytoplasmic domain (Holm et al., 1996). CHL1 is a strong promoter of neurite outgrowth in vitro and may bind homophilically as well as heterophilically (Hillenbrand et al., 1999). CHL1 knockout mice display aberrant guidance of olfactory axons and hippocampal mossy fibers, and these mice are defective in cognitive processing of spatial information (Montag-Sallaz et al., 2002) and attention (Pratte et al., 2003). In humans, mutations in the *CHL1* gene ortholog, *CALL*, are associated with the human 3p syndrome, which is characterized by mental retardation or low IQ, and delayed speech and motor development (Angeloni et al., 1999; Frints et al., 2003). L1 mutations induce a mental retardation syndrome that is more complex than the 3p syndrome and may cause spasticity, corpus callosum agenesis, and optic atrophy (Kenwrick et al., 2000). Many of these features are phenocopied in L1 knockout mice (Cohen et al., 1997; Dahme et al., 1997; Demyanenko et al., 1999, 2001; Demyanenko and Maness, 2003). Polymorphisms in both the *CHL1/CALL* and *L1* genes have been linked to increased risk for schizophrenia (Kurumaji et al., 2001; Sakurai et al., 2002). These findings suggest a role for CHL1 in human brain development and function, but cortical abnormalities in CHL1-minus mice have not yet been identified.

Migration of cortical neurons to their final location in the cerebral cortex and the ensuing development of dendrites and axons are fundamental processes in the formation of the cerebral cortex. The neocortical region of the brain is comprised of distinct areas with a common organization but with different functions and patterns of neuronal connectivity. An important goal is to elucidate the molecules and mechanisms that govern cortical area-specific neuronal differentiation. Transcription factors with graded expression in the embryonic cortex are required for normal patterning (Marin and Rubenstein, 2003), but less is known about area-specific guidance molecules for migrating neurons, whose expression may be governed by such factors. *CHL1* emerged in a screen for genes differentially expressed in the caudal versus rostral neocortex of the rat (Liu et al., 2000). CHL1 mRNA was localized in a spatially and temporally graded pattern in migrating neuronal precursors and in differentiating, postmitotic pyramidal neurons enriched in layer V (Hillenbrand et al., 1999; Liu et al., 2000). The graded pattern of CHL1 expression suggested a function in cortical area-specific development.

Based on these results, we undertook an investigation to examine a potential role for CHL1 in development of cortical pyramidal neurons in the mouse neocortex. We anticipated that CHL1 might modulate cortical neuron migration, because we had shown that expression of CHL1 in transfected HEK293 cells strongly potentiates haptotactic migration to extracellular matrix proteins

*Correspondence: srclab@med.unc.edu

in vitro (Buhusi et al., 2003). Moreover, the stimulation of migration by CHL1 in these cells is dependent on integrins, which have been implicated in cortical neuron adhesion and migration (Anton et al., 1999; Dulabon et al., 2000; Sanada et al., 2004). Here, we identify a cortical area-specific role for CHL1 in modulating radial migration and apical dendrite development of pyramidal cells.

## Results

### CHL1 Exhibits Graded Expression in Developing Cortical Pyramidal Neurons

To assess a potential role of CHL1 in migration and differentiation of cortical neurons along the rostrocaudal axis, the pattern of expression and localization of CHL1 protein was analyzed in the developing cerebral cortex of the mouse. Immunofluorescence staining showed that CHL1 was expressed at highest levels in the caudal cortex and lower levels in the rostral cortex at E14.5 during migration of neuronal progenitors from the ventricular zone to the cortical plate (Angevine and Sidman, 1961) (Figures 1A and 1B). Staining was most prominent in the intermediate zone, which contains radially and tangentially migrating precursors as well as corticofugal axons from subplate and cortical plate neurons. At higher magnification, cells in the intermediate zone distinct from axons were clearly labeled with CHL1 antibodies (Figure 3O, arrows). Lower levels of CHL1 were seen in the cortical plate and marginal zone, but little was observed in proliferating progenitors of the ventricular zone. CHL1 did not colocalize with the radial glial marker RC2 in the ventricular zone (data not shown), indicating that it was not in radial glia.

At E17, deep layer pyramidal neurons (V/VI) accumulate in the cortical plate, where they extend axonal and dendritic processes, while some neurons destined for the upper layers continue to migrate (Angevine and Sidman, 1961). At this stage, CHL1 displayed a graded pattern of expression with highest levels caudally in the future visual cortex, moderate levels in the somatosensory region, and low levels rostrally in the motor region (Figures 1C–1F). In the posterior cortical regions, CHL1 was most evident in the cortical plate and subventricular zone (Figures 1E–1F).

By postnatal day 0 (P0), when all cortical layers are present, CHL1 declined throughout the cerebral wall but still exhibited graded expression along the rostrocaudal axis (Figures 1G–1I). Strongest staining was observed in the visual cortex (Figure 1I), where it was more pronounced in layers V/VI than in layer II/III. Layer I staining may be due to CHL1 in axons or apical dendritic tufts. Moderate levels were seen in the somatosensory cortex, and staining in the motor cortex was mostly restricted to layer I. Control staining with nonimmune IgG was negative (Figure 1J), and staining of the CHL1-minus cortex with CHL1 antibody was minimal (shown for P0 in Figure 1K). Double immunofluorescence staining of E17 and P0 visual cortex for CHL1 and the neuronal somatodendritic marker MAP2 (microtubule-associated protein 2) showed CHL1 expression in pyramidal neurons, localizing to somata and apical dendrites (Figures 1M–1P, arrows), and in the apical pole of pyramidal cells (Figures 1Q–1S, arrows). The pattern of CHL1 protein expression was in accord with in situ hybridization data, which showed a rostrocaudal gradient of CHL1 mRNA expression in postmitotic neurons during rat neocortical development (Liu et al., 2000). The CHL1 antibody recognized full-length CHL1 (185 kDa) and a small amount of a 165 kDa cleavage fragment in E14.5 brain (Figure 1L), the levels of which declined in 4-week-old mice (Holm et al., 1996; Hillenbrand et al., 1999).

The spatiotemporal pattern of CHL1 expression was consistent with an onset in postmitotic migratory precursors in posterior cortical areas, persisting at lower levels in pyramidal neurons during postnatal development.

### Altered Neuronal Distribution and Misorientation of Apical Dendrites in Layer V Pyramidal Cells of CHL1-Minus Mice

Homozygous mice lacking the CHL1 gene showed no gross defects in cortical lamination by Nissl staining (Figures 1T and 1U). All layers of the neocortex of adult mutants were present in roughly the same order as wild-type, and heterotopias were not observed. However, subtle differences in neuronal distribution could be discerned in posterior neocortical areas, where there was a blurred distinction between layers, indicated between layers IV and V (Figure 1U, arrowhead).

To investigate cortical defects, CHL1 mutant mice were intercrossed with a reporter strain in which layer V pyramidal neurons are intrinsically labeled with enhanced yellow fluorescent protein (YFP) expressed from the Thy-1 promoter (Thy1/YFP line H) (Feng et al., 2000). Expression of YFP is initiated in a subpopulation of layer V pyramidal neurons in the first few postnatal weeks and persists into adulthood, filling cell soma, dendrites, and axon shafts (Feng et al., 2000). Examination of serial sagittal and coronal sections of wild-type Thy1/YFP mice (line H) at postnatal day 28 showed that layer V pyramidal neurons expressed YFP prominently throughout the neocortex except in the primary visual cortex (v1), where labeling was low.

In the motor cortex, YFP-labeled layer V pyramidal neurons of CHL1-minus mice were indistinguishable from wild-type mice in distribution and morphology (Figures 2A and 2D). Layer V neurons were distributed in a broad band, their apical dendrites ascending directly to layer I, where they branched to form apical tufts. In the somatosensory cortex, where the level of CHL1 expression was intermediate, the laminar distribution of YFP-labeled pyramidal neurons of CHL1-minus mice was similar to wild-type, but their apical dendrites assumed a wavy, misoriented trajectory, ultimately reaching layer I, where they formed apical tufts (Figures 2B and 2E).

The most prominent defects were observed in the mutant secondary visual cortex (v2 region), where CHL1 was normally expressed at highest levels and YFP labeling was robust (Figures 2C, 2F, and 2G). Numerous YFP-labeled neurons were displaced to layer VI (Figure 2F, arrowheads). The displaced mutant neurons frequently exhibited apical dendrites with an inverted morphology, oriented sideways or toward the ventricular surface (Figure 2F, arrowheads). Occasionally, inverted pyramidal cells were observed in wild-type visual cortex (Figure 2C, arrowhead) as reported (Miller, 1988), but they were 8-fold more abundant in CHL1 mutants (discussed below; Figure 4). At higher magnification, CHL1 mutant pyramidal neurons in layer VI could be seen to have

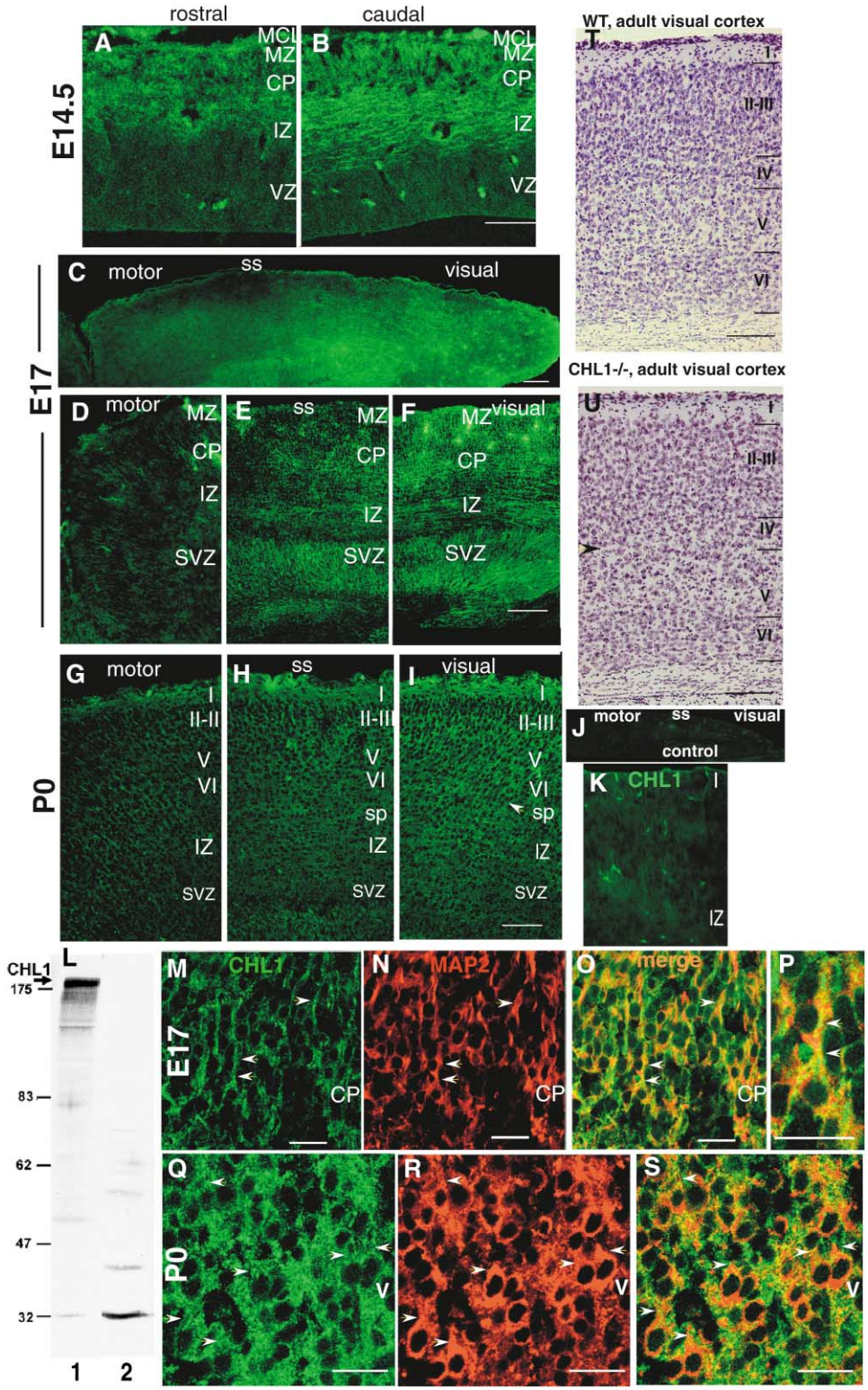


Figure 1. CHL1 Expression in the Developing Neocortex

Immunofluorescence staining for CHL1 in (A and B) coronal and (C–I) medial sagittal sections of the developing wild-type mouse neocortex visualized by confocal microscopy. (J) Nonimmune IgG staining at E17. (K) Control staining of CHL1-minus visual cortex at P0 with CHL1 antibody (compare to [I]). (L) Western blot of E14.5 brain (40 μg) with (1) CHL1 antibody or (2) normal IgG. Arrow shows 185 kDa CHL1 protein. (M–S) Double immunofluorescence staining for CHL1 and MAP2 in visual cortex. Arrows in (M)–(P) show colocalization in apical dendrites of pyramidal cells. Arrows in (Q)–(S) show localization in apical pole of pyramidal cell somata. (T and U) Nissl staining of adult visual cortex of wild-type and CHL1 mutant mice. Arrow in (U) points to blurred border between layers IV and V. Motor, motor cortex; ss, somatosensory cortex; visual, visual cortex; MCL, meningeal cell layer; MZ, marginal zone; CP, cortical plate; IZ, intermediate zone; VZ, ventricular zone; SVZ, subventricular zone. Scale bars, 100 μm in (A)–(I), (T), and (U) and 20 μm in (M)–(S).

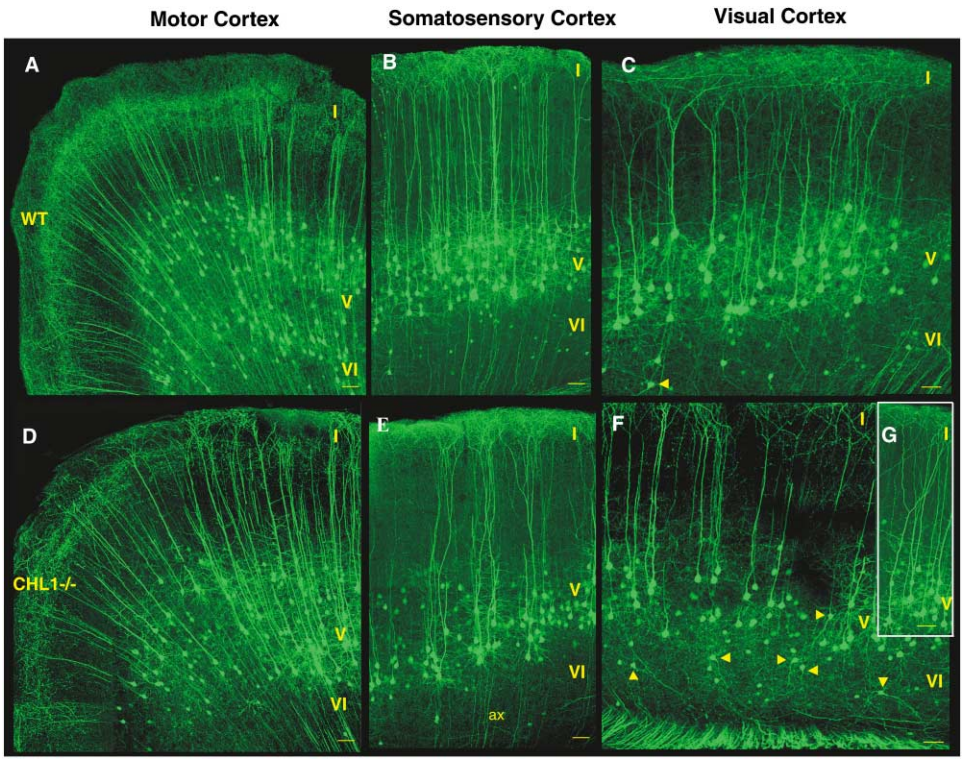


Figure 2. Altered Neuronal Distribution and Misorientation of Apical Dendrites in CHL1-Minus Mice Expressing YFP in Layer V Pyramidal Cells

Location and morphology of YFP-labeled neurons in sagittal sections of the motor, somatosensory, and visual cortex (v2) of wild-type (A–C) and CHL1-minus (D–G) littermates (P21–P28). Arrows point to neurons displaced to layer VI displaying misoriented apical dendrites. I–VI, cortical layers; ax, axon. Scale bars, 50 μm.

apical dendrites emerging from somata, which also appeared inverted with the narrower end pointed downward (Figures 3A and 3B, arrows). The thick apical dendrite-like process resembled a dendrite in every respect but orientation, developing branches and spines. Inverted neurons developed basal dendrites that resembled wild-type. The axons of these neurons emerged from the lower surface of inverted somata in a generally normal direction. Inverted apical dendrites, as well as basal dendrites of mutant pyramidal cells, developed spines that were indistinguishable from wild-type in terms of morphology (mushroom spines) and density (Figures 3C and 3D). Basal dendrites had equivalent mean spine densities in wild-type ($0.27 \pm 0.02$ spines/μm; $n = 1265$ spines) and CHL1-minus cortex ($0.24 \pm 0.02$ spines/μm; $n = 961$ spines) (Student's t test; $p < 0.05$); however, a more detailed analysis is required to assess dendritic branching and spine morphology.

To verify that YFP-labeled neurons in layer VI of the CHL1-minus visual cortex were displaced layer V cells, 5-bromo-2′-deoxyuridine (BrdU) labeling was carried out at E13.5, when many deep layer cells (V/VI) are born (Chae et al., 1997). The final position of neurons was analyzed postnatally by BrdU immunostaining. Wild-type $YFP^+$ neurons labeled with BrdU were mostly present in layer V (Figures 3I–3K). CHL1-minus $YFP^+$ neurons labeled with BrdU were seen in layer VI as well as layer V (Figures 3E–3G, arrows) and showed inverted apical dendrites in layer VI (Figure 3H, arrow). Er81 is a transcription factor specific for subpopulations of layer V pyramidal cells throughout the postnatal mouse neocortex, including callosal and subcortical projection neurons (Hevner et al., 2003). To further ascertain that YFP+ neurons in layer VI of the mutant visual cortex were displaced layer V cells, immunostaining was carried out with an antibody specific for Er81 (Jessell, 2000). Most $YFP^+$ neurons in layer V of the wild-type visual cortex were Er81 positive; a few $YFP^+$ cells in layer VI did not express Er81 (Figures 5A–5C). In the CHL1 mutant visual cortex, $YFP^+$ neurons in layer V as well as layer VI expressed Er81, including cells with a clearly inverted morphology (Figures 5D–5F, arrows). Thus, YFP-labeled cells that were displaced to layer VI in CHL1 mutant visual cortex had properties of layer V pyramidal neurons.

To quantitatively compare the distribution of YFP-positive pyramidal neurons of CHL1-minus and wild-type littermates (P21–P28), neurons were grouped into bins according to their migration index, presenting the distance of neurons from the white matter relative to cortical thickness. In the CHL1-minus visual cortex (v2), there was a large increase in the percent of cells in the lowest bin (bin 1) and a corresponding decrease in bins 2 and 3 (Figure 4A). The distributions of CHL1-minus neurons in the motor and somatosensory cortex were not significantly different from wild-type. No differences were observed in cortical thickness of wild-type versus CHL1-minus mice in any cortical area (data not shown).

To characterize the laminar distribution of pyramidal neurons in the lowest bin of the visual cortex in a separate experiment, $YFP^+$ cells were scored in layers V and VI, the boundary between which was distinguished by

immunostaining with Er81 antibody in wild-type sections. The percentage of YFP$^+$ cells in the equivalent layer VI region of the CHL1-minus visual cortex (41% $\pm$ 0.01%; n = 562 cells; two mice) was significantly greater than in wild-type (13% $\pm$ 0.01%; n = 347 cells; two mice) (Student's t test; $p < 0.05$). Thus, the redistribution of YFP$^+$ neurons in CHL1-minus visual cortex into layer VI corresponded well to the altered distribution in bin 1.

To quantitate the misprojection of apical dendrites of YFP-labeled pyramidal neurons in the CHL1-minus cortex, the direction of apical dendrites was measured as an angle of orientation ($\theta$) relative to the pial surface (Figure 4B, diagram). In each area of the wild-type cortex, 80%–90% of neurons had apical dendrites that were normally oriented within the shaded area of the diagram ($|\theta| \leq 6°$). Neurons with apical dendrites that projected outside this normal range ($|\theta| > 6°$) were significantly increased in the CHL1-minus somatosensory and visual cortex but not motor cortex (Figure 4C). Within this group, neurons with inverted dendrites ($|\theta| > 90°$) were also increased in the CHL1-minus somatosensory and visual cortex but not motor cortex (Figure 4D). These results were consistent with caudal area-specific regulation of dendritic orientation by CHL1. Golgi impregnation was carried out to evaluate whether dendritic misorientation occurred in other layers of the mutant visual cortex. Many Golgi-stained neurons with inverted morphology could be seen in layers VI and V of the CHL1-minus visual cortex (Figure 5M, arrows) but not in layers II/III. These results suggested that loss of CHL1 affects dendritic orientation in the visual cortex primarily in deeper cortical layers.

### Loss of CHL1 Shifts the Radial Distribution of Callosal and Corticotectal Neurons but Does Not Affect Cell Survival or Posterior Areal Boundaries

Many YFP-labeled neurons that were displaced to deeper levels in the CHL1-minus visual cortex (v2) were of small diameter (Figure 3A, small arrows), but some large diameter neurons were also displaced (Figures 3A and 3B, large arrows). In the rodent visual cortex, many small diameter pyramidal cells project callosally and are located in the deeper part of layer V, whereas large diameter pyramidal cells project subcortically to the superior colliculus and lie more superficially in layer V (Koester and O'Leary, 1992; Kasper et al., 1994).

To determine if the distribution of callosally projecting pyramidal neurons in layer V was altered in CHL1 mutants, injections of DiI were made into the visual cortex of wild-type and CHL1 mutant littermates at P5 to retrogradely label callosally projecting pyramidal cells in the contralateral visual cortex as well as neurons in the ipsilateral cortex with intrahemispheric connections. In the contralateral visual cortex (v2) of wild-type mice at P7, DiI-labeled callosal neurons were prominent in layer II/III, substantial in layer V, but less common in layers IV and VI (Figure 5G) as in the rat (Kasper et al., 1994). CHL1-minus-labeled callosal neurons showed a broader distribution with more cells in layers VI and IV (Figure 5H). Many layer VI cells had inverted morphologies (Figure 5I). The percent of DiI-labeled callosal neurons in layer VI was significantly greater in mutant (12.5% $\pm$ 0.02%; n = 93 cells) than wild-type (6.2% $\pm$ 0.04%; n = 35 cells) (Student's t test; $p \leq 0.05$; three mice per genotype). A downward shift in position of DiI-labeled callosal neurons in the middle layers (III/IV) was also evident in CHL1 mutants (Figure 5H), suggesting an effect on other populations of neurons as well. No differences were apparent in the distribution of intrahemispherically connected DiI-labeled neurons in the visual cortex of mutants (data not shown). Thus, small cells displaced to layer VI in the CHL1-minus visual cortex were callosally projecting pyramidal neurons, most likely from layer V.

DiI injections were also made into the superior colliculus of wild-type and CHL1 mutants at P2 to retrogradely label corticotectal pyramidal cells, which are normally located in upper layer V of the visual cortex. DiI-labeled neurons in the visual cortex (v2) at P4 were found predominantly in layer V of both genotypes (Figures 5J and 5K); however, the distribution of neurons in CHL1 mutants was shifted downward. The resulting migration index was significantly lower for CHL1-minus pyramidal cells (0.45 $\pm$ 0.01 $\mu$m; n = 155 cells) compared to wild-type cells (0.50 $\pm$ 0.01 $\mu$m; n = 83 cells) (Student's t test, $p < 0.05$), suggesting that corticotectal pyramidal cells in the CHL1-minus visual cortex also assumed a deeper position than wild-type neurons. DiI-labeled corticotectal neurons did not display an inverted morphology.

CHL1 can prevent death of cerebellar granule neurons and hippocampal neurons in vitro (Chen et al., 1999). To assess whether there was any loss of pyramidal neurons in the CHL1-minus neocortex, the density of YFP-labeled cells was measured in level-matched sections. There was no significant difference in the density of small ($<$18 $\mu$m) or large diameter ($\geq$18 $\mu$m) neurons in cortex of CHL1 mice compared to littermate controls (Table 1). A trend toward fewer large diameter neurons in each cortical area of the mutants was not statistically significant. Thus, although apoptosis was not directly assayed, there appeared to be no loss of pyramidal cells in any region of the CHL1-minus cortex.

The posterior phenotype of the CHL1-minus cortex raised the possibility that the abnormal distribution of YFP$^+$ pyramidal cells in layer VI reflected or resulted from a shift in the boundaries of posterior cortical areas. We were able to test this hypothesis by making use of the fact that layer V pyramidal neurons of Thy1/YFP mice (line H) expressed YFP strongly in the secondary visual cortex (v2) but not in the primary visual cortex (v1), providing a fluorescent marker for the boundary between these cortical subregions. Examination of serial coronal sections of the neocortex of two YFP$^+$ wild-type and three CHL1 littermates revealed no differences in these boundaries, which were equidistant from the midline at every matched rostrocaudal level. The overall sizes of the mutant and wild-type brains were similar. Thus, CHL1 loss did not affect the cortical area boundary, leading us therefore to test the hypothesis that CHL1 regulated radial migration of cortical precursors.

### Analysis of Cortical Neuron Migration by BrdU Labeling

To evaluate the effect of CHL1 on laminar positioning of pyramidal neurons in the visual cortex, BrdU injections were made in vivo at E11.5 to preferentially label subplate and some layer VI neurons (Rice et al., 1998); at

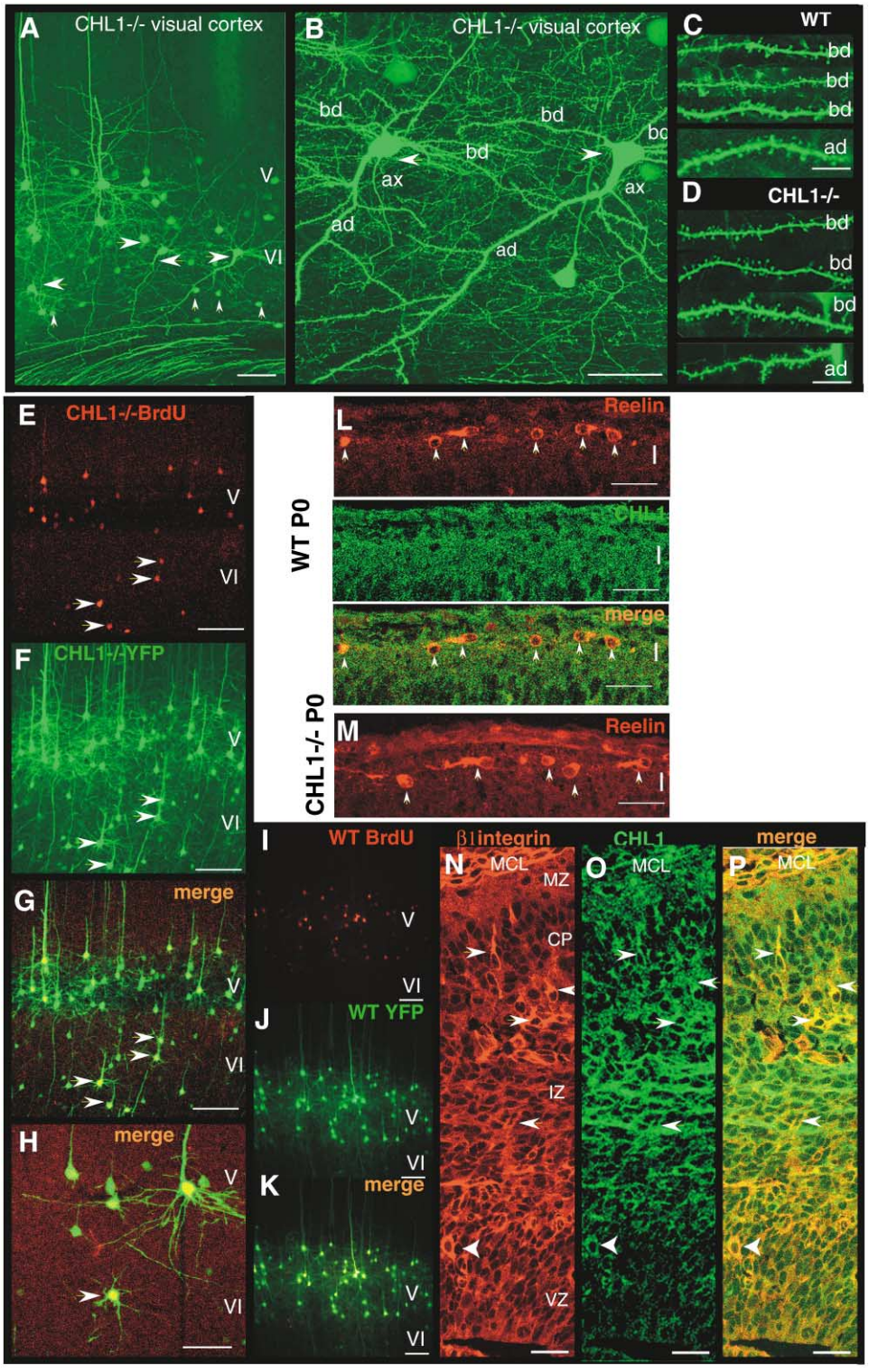


Figure 3. Inverted Apical Dendrites of CHL1-Minus Pyramidal Cells and Colocalization of CHL1 with β1 Integrins in the Visual Cortex

(A) Inverted apical dendrites of large diameter (≥10 μm; large arrows) and small diameter (>18 μm; small arrows) YFP-labeled pyramidal cells displaced to layer VI in CHL1-minus visual cortex. Scale bar, 50 μm.

(B) High magnification of large diameter cells in (A) (arrows) showing misoriented apical dendrites (ad) with normal dendritic spines, basal dendrites (bd), and normally oriented axons (ax). Scale bar, 50 μm.

(C and D) Dendritic spines along basal dendrites (bd) and apical dendrites (ad) of displaced YFP-labeled pyramidal cells in CHL1-minus mice were similar to those of layer V neurons of wild-type (WT) mice. Scale bar, 5 μm.

(E–K) Many displaced YFP-labeled CHL1-minus pyramidal neurons (arrows) were born at the same time (E13.5) as wild-type layer V neurons.

(E) Distribution of CHL1-minus neurons immunostained for BrdU. BrdU labeling was carried out at E13.5, and neuronal position was analyzed

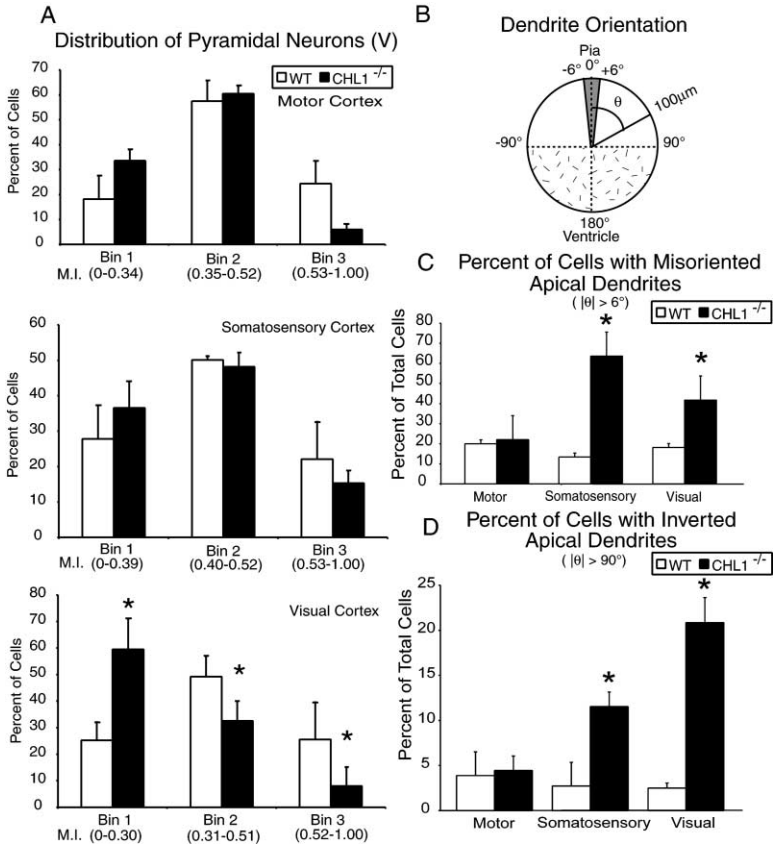


Figure 4. Quantification of Aberrant Location and Dendrite Projections of YFP-Labeled Pyramidal Neurons in the Motor, Somatosensory, and Visual Cortex of CHL1-Minus Mice

(A) Distribution of YFP-labeled pyramidal neurons in the cortex of wild-type ($n = 4$) and CHL1-minus ($n = 4$) littermates (P21–P28). The migration index (M.I.) was determined for 257 to 573 neurons per genotype and region. Significant differences (asterisks) in the percent of wild-type and mutant cells in each bin were determined by the Mann-Whitney rank sum test; $p < 0.05$.

(B) Scoring method for apical dendrite orientation (see Experimental Procedures).

(C) The percent of cells with misoriented apical dendrites (including inverted dendrites) was increased in the somatosensory and visual cortex of CHL1 mutants. The number of cells ranged from 98 to 283 for each genotype and region. Two to four mice of each genotype were analyzed. Significant differences (asterisks) in wild-type and mutant dendrites were determined by the Student's t test ($p < 0.05$).

(D) The percent of cells with inverted apical dendrites was increased in the somatosensory and visual cortex of CHL1 mutants. The number of dendrites ranged from 165 to 853 for each genotype and region. Three to eight mice of each genotype were analyzed. *Statistically significant difference (±SE) (Student's t test; $p < 0.05$).

E13.5 to preferentially label layer IV, layer V, and to some extent layer VI neurons (Chae et al., 1997); and at E14.5 to preferentially label superficial layer and some middle layer neurons (Cahana et al., 2001). Distribution of labeled cells was analyzed at P0. Cells labeled at E11.5 in the CHL1 mutant cortex were seen to split the preplate normally but were somewhat more deeply displaced than wild-type (Figures 6A–6C). The deeper layer neurons labeled at E13.5 in the CHL1 mutant cortex also occupied lower than normal positions in the cortical plate (Figures 6E–6G). Moreover, there was a clear accumulation of labeled neurons within the intermediate zone, consistent with a delay in migration. These cells expressed the neuronal marker TuJ1$^+$ (data not shown) and thus were not proliferative progenitors. Neurons labeled at E14.5 were less affected in their positioning within the upper and to a lesser extent middle layers of the CHL1 mutant cortex but did display a small but significant degree of malpositioning (Figures 6I–6K). CHL1 mutant neurons labeled on E14.5 were also abnormally prevalent in the intermediate and ventricular/subventricular zones (Figures 6J and 6L), suggesting a delay in migration of upper or middle layer neurons. This may be due to loss of CHL1 from these neurons or an indirect consequence of altered positioning and dendritic development of deep layer neurons. Neurons labeled at E13.5 or E14.5 were no longer apparent at these sites by P21 (data not shown), suggesting that they either reached their destination in the cortex or died. Overall, these results were consistent with an impairment in radial migration of deep layer neurons, with delay in migration of some middle or superficial layer neurons in the CHL1 mutant visual cortex.

### Loss of CHL1 Decreases the Rate of Radial Migration of Neurons in Cortical Slices

To further investigate whether CHL1 modulated radial migration of cortical neurons, the rate of neuronal move-

at P21. Arrows show labeled neurons displaced to layer VI. (F) YFP fluorescence image of section in (E) with arrows pointing to displaced neurons. (G) Merged images (E and F) showing convergence of BrdU labeling and YFP fluorescence in displaced neurons with normal dendrites. (H) Merge of a different region showing convergence of BrdU labeling and YFP fluorescence in a displaced neuron with inverted morphology (arrow). Scale bars, 100 μm in (E)–(G) and 50 μm in (H). (I) Distribution of wild-type YFP$^+$ neurons labeled with BrdU at E13.5 and analyzed at p21. Labeled neurons are seen in layer V. (J) YFP fluorescence image of section in (I). (K) Merged images (I and J) showing convergence of BrdU labeling and YFP fluorescence in pyramidal neurons in layer V. Scale bars, 100 μm (I–K).

(L) Double immunofluorescence staining in visual cortex (layer I) of wild-type P0 mice shows labeling of reelin but not CHL1 in Cajal-Retzius neurons (arrows). Scale bar, 10 μm.

(M) Cajal-Retzius cells (arrows) stained for reelin are not altered in CHL1-minus visual cortex. Scale bar, 10 μm.

(N–P) β1 integrin and CHL1 colocalize (arrows) in the developing caudal neocortex during neuronal migration. Immunofluorescence staining of the caudal neocortex of wild-type mice at E14.5 for β1 integrin (N) and CHL1 (O) and merge (P). Scale bars, 20 μm (N–P).

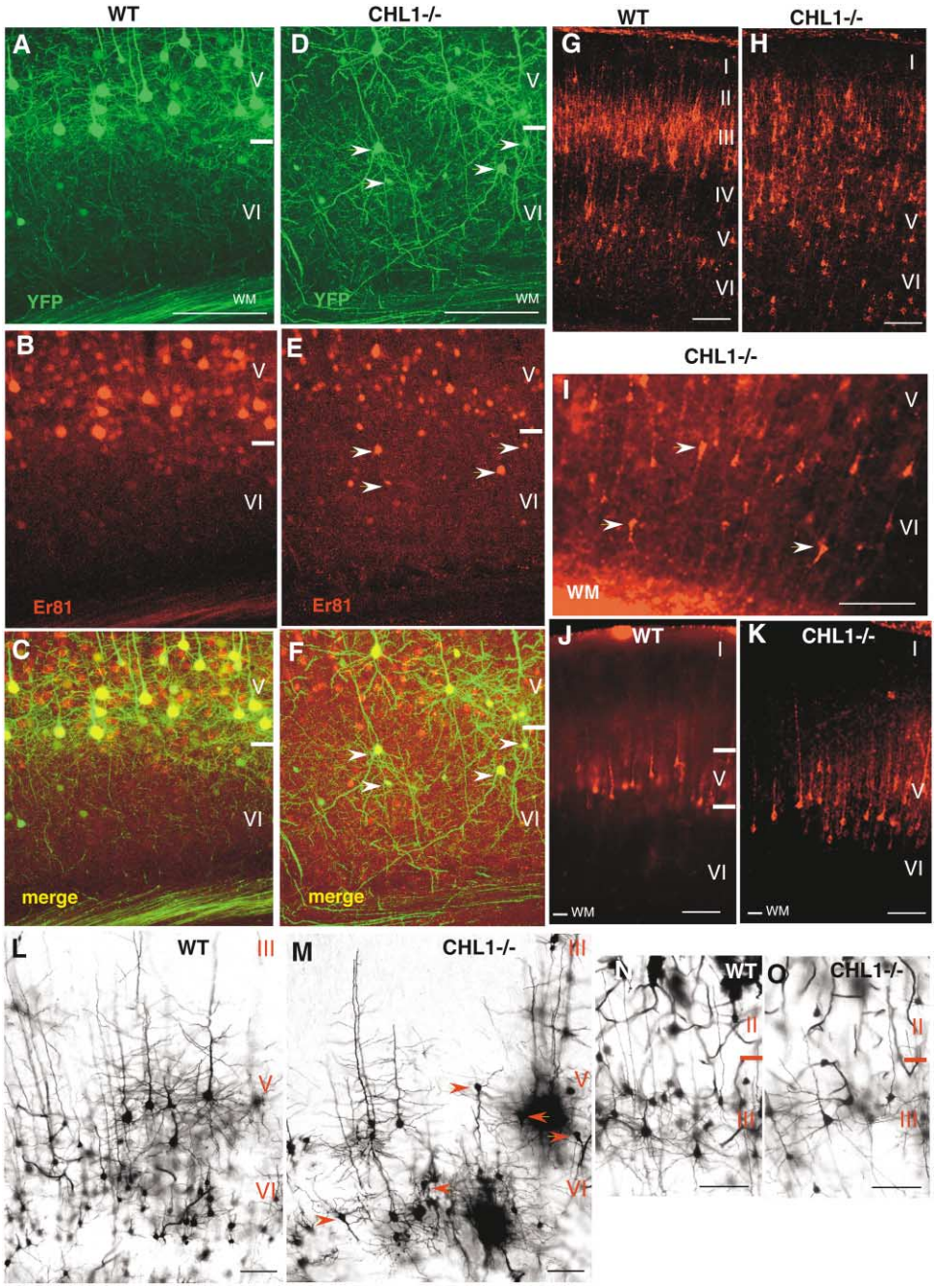


Figure 5. Identification of Displaced Pyramidal Neurons in CHL1-Minus Visual Cortex

(A–F) Colocalization of Er81 transcription factor, a marker of layer V pyramidal cells with YFP in pyramidal neurons displaced to layer VI in the visual cortex of CHL1 mutant mice. (A and D) YFP fluorescence in wild-type (WT) and *CHL1*$^{-/-}$ visual cortex. (B and E) Er81 indirect immunofluorescence staining. (C and F) Merge of images. Arrows show double-labeled cells with misoriented apical dendrites in layer VI and lower layer V. Scale bar, 100 μm.

(G–I) Altered distribution of callosally projecting neurons in CHL1-minus visual cortex. Callosally projecting neurons were retrogradely labeled with DiI from the visual cortex at P5 and analyzed in the contralateral visual cortex at P7 in three wild-type and four CHL1 mutant mice. (I) Many mutant neurons in layer VI close to the white matter (WM) had inverted dendrites (arrows). Scale bars, 100 μm.

(J–K) Altered distribution of corticotectal neurons in CHL1-minus mice. Corticotectal neurons were retrogradely labeled with DiI from the superior colliculus at P2 and analyzed at P4 in the visual cortex of four wild-type and four CHL1 mutant mice. CHL1-minus neurons within layer V were shifted toward the white matter (WM). Scale bars, 100 μm.

(L–O) Apical dendrite inversion and misorientation in Golgi-stained pyramidal neurons located in deep but not upper layers of the CHL1-minus visual cortex. Pyramidal cells with misoriented apical dendrites in layers V and VI of wild-type (L) and CHL1-minus visual cortex (M). (N and O) Normal morphology of CHL1-minus neurons in layers II and III. Scale bars, 50 μm.

Table 1. Density of Layer V Pyramidal Neurons Is Unaltered in *CHL1*$^{-/-}$ Mice

| | Mean Neuronal Density (cells/mm$^2$)[a,b] | | | |
|---|---|---|---|---|
| | Somata $< 18$ μm | | Somata $\geq 18$ μm | |
| Cortical Area | Wild-Type | *CHL1*$^{-/-}$ | Wild-Type | *CHL1*$^{-/-}$ |
| Motor | 25 ± 2 | 39 ± 10 | 112 ± 15 | 92 ± 13 |
| Somatosensory | 20 ± 2 | 28 ± 4 | 97 ± 19 | 66 ± 16 |
| Visual | 64 ± 1 | 55 ± 7 | 44 ± 7 | 30 ± 5 |

[a] Data were obtained from five to seven mice of each genotype (200 to 500 cells per mouse).
[b] Differences in neuron density or cortical thickness were not significant in any cortical area between wild-type and *CHL1*$^{-/-}$ mice ($p < 0.05$; two-tailed Student's t test).

ment was measured in acute brain slice cultures from wild-type and CHL1-minus embryos at E14.5, when pyramidal cell precursors destined for layers V/VI migrate to the cortical plate. Caudal brain sections containing the visual cortex were incubated briefly in culture (1 hr) with Oregon Green BAPTA-1 488AM, which randomly labels neurons through the slices and allows visualization of their movement, as described by others (Nadarajah et al., 2001, 2003; Nadarajah and Parnavelas, 2002). The next day, cell migration was measured by time-lapse confocal videomicroscopy. Neurons in wild-type and mutant slices were labeled equivalently with BAPTA 488 (Figures 7B and 7C). Moreover, radially migrating neurons in CHL1-minus slices displayed shorter and thinner radially directed leading processes than wild-type neurons (Figures 7B and 7C, arrows). In addition, the somata of these CHL1-minus neurons were rounded and did not exhibit the elongated morphology of wild-type cells actively migrating on glial guides. The locations of individual cell somata in the intermediate zone were measured every 10 min for 3 hr. Only cells moving radially through the intermediate zone were analyzed, although some tangential, oblique, and ventricle-directed migration was seen. Notably, CHL1-minus neurons exhibited a strikingly slower rate of radially oriented somal movement than wild-type neurons (Figures 7B and 7C). The radial displacement of somata for a typical wild-type and CHL1-minus neuron had very different kinetics (Figure 7D). The average speed of somal movement for the two populations was estimated by measuring the total somal displacement in 2 hr (Figure 7E). The average somal speed for neurons lacking CHL1 (3.31 ± 0.17 μm/hr; $n = 55$) was approximately 25% of wild-type (12.65 ± 1.29 μm/hr; $n = 53$). Approximately, the same difference in rates was obtained regardless of whether the cells were in the lower, middle, or upper third of the intermediate zone (data not shown). The average migratory speed of wild-type neurons was within the range reported for neurons in early embryonic brain slices (Komuro and Rakic, 1992; Takahashi et al., 1996; Nadarajah et al., 2001). These findings demonstrated that the radial migration of deep layer cortical neurons lacking CHL1 was significantly slower than that of wild-type neurons in cortical slices.

A loss or altered distribution of Cajal-Retzius cells in layer I might indirectly affect radial migration through deficits in reelin expression. To determine if Cajal-Retzius cells in wild-type mice expressed CHL1, double staining was carried out for CHL1 and reelin in the visual cortex at P0. Cells in layer I with horizontal morphology typical of Cajal-Retzius cells were strongly labeled with reelin antibodies but were not reactive with CHL1 antibodies (Figure 3L, arrows), indicating that Cajal-Retzius neurons did not express CHL1. Furthermore, the CHL1-minus visual cortex displayed no loss or morphological alteration of Cajal-Retzius neurons revealed by reelin immunostaining (Figure 3M). Thus, the aberrant migration and laminar distribution of CHL1-minus pyramidal neurons in the posterior neocortex were not attributable to abnormal reelin expression.

### Loss of CHL1 Decreases Integrin-Dependent Haptotactic Migration of Cortical Neurons

Haptotactic cell migration in Transwells provides a useful model to study cortical neuron migration. Dissociated cortical neurons from the caudal brain regions of wild-type and CHL1-minus embryos (E14.5) were assayed for migration toward fibronectin in Transwell assays. Fibronectin may play a role in neuronal migration in the cortex, as it is expressed by migrating neurons and is associated with radial glial processes (Sheppard et al., 1991; Sheppard and Pearlman, 1997; Stettler and Galileo, 2004). Wild-type cortical neurons migrated robustly toward fibronectin, whereas random migration toward poly-D-lysine was much lower (Figure 7A). In contrast, cortical neurons lacking CHL1 migrated more slowly to fibronectin. Function-blocking antibodies against β1 or α3 integrin effectively inhibited cortical neuron migration to fibronectin but had no further effect on migration of CHL1-minus neurons. Nonimmune immunoglobulin and irrelevant antibodies against αvβ3 integrin did not perturb migration of wild-type or mutant neurons. As for cortical neurons, CHL1 also potentiated migration of HEK293 cells to fibronectin, which was completely inhibited by α3 or β1 integrin antibodies (data not shown). Recombinant reelin as a substrate did not support haptotactic migration of CHL1-expressing HEK293 cells (data not shown) or B35 rat neuroblastoma cells (Thelen et al., 2002). Thus, CHL1 has the potential to promote embryonic cortical neuron migration through α3β1 integrins.

To determine whether CHL1 and β1 integrins colocalized in migrating neuronal precursors, expression of β1 integrins and CHL1 was assessed in the caudal neocortex of wild-type mouse embryos at E14.5 by double immunofluorescence staining (Figures 3N–3P). Subpopulations of cells with an elongated, radially oriented morphology characteristic of migrating neurons coexpressed CHL1 and β1 integrins in the upper ventricular zone, intermediate zone, and lower cortical plate (arrows). β1

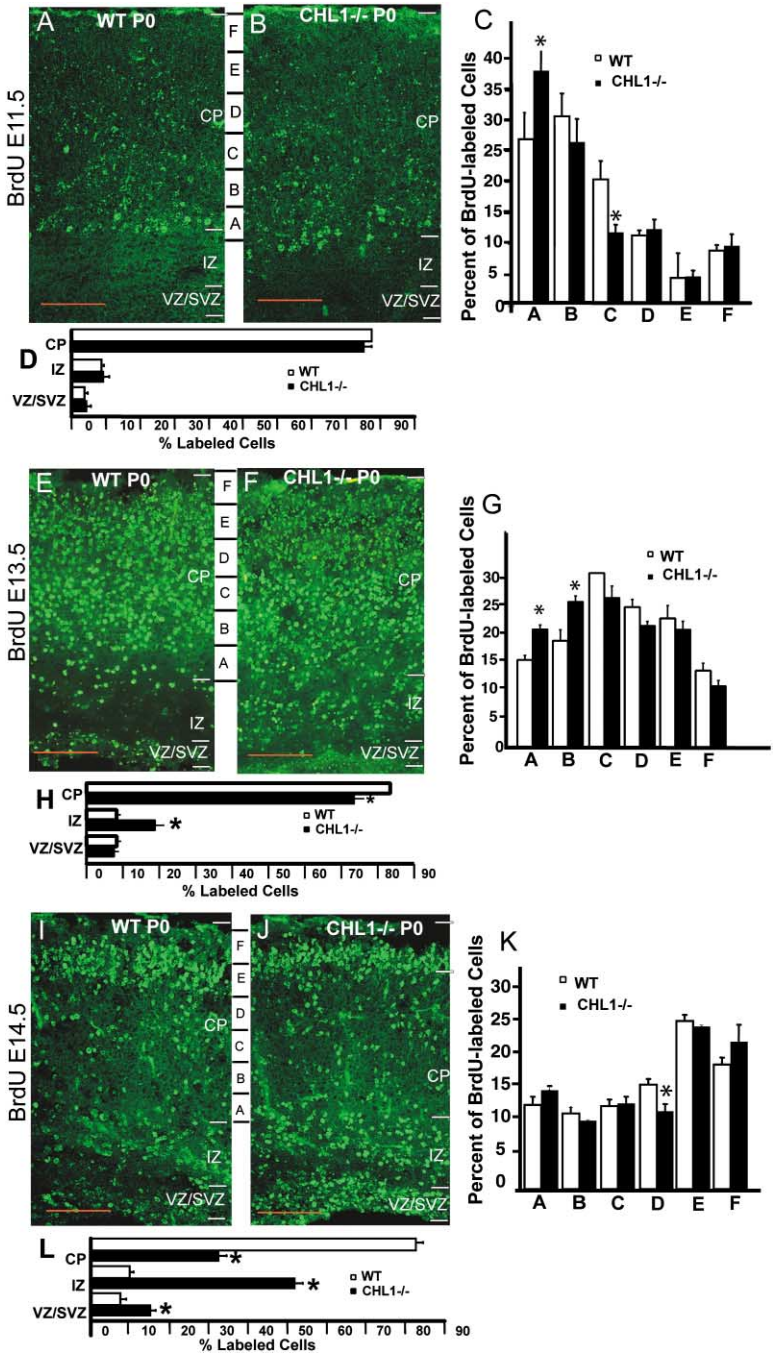


Figure 6. In Vivo Analysis of Neuronal Migration

Neurons from wild-type and CHL1-minus littermates were labeled with BrdU at E11.5 (A and B), E13.5 (E and F), and E14.5 (I and J); then laminar distribution was analyzed at P0 by immunostaining for BrdU. The cortex was divided into six equal sectors (A–F), and the percent of labeled cells in each sector was separately determined (C, G, and K). The percent of labeled cells was compared in the cortical plate (CP), intermediate zone (IZ), ventricular zone (VZ), and subventricular zone (SVZ) (D, H, and L).

integrin staining was not completely coincident with CHL1, but it was broadly distributed throughout the cerebral wall, in agreement with in situ hybridization (Graus-Porta et al., 2001), whereas CHL1-positive afferents within the intermediate zone did not coexpress β1 integrins. Thus, CHL1 was expressed at the appropriate time and place to interact with β1 integrins in migrating cortical neurons.

## Discussion

Here, we identify a novel role for CHL1 in cortical neuron positioning and dendritic projection in the posterior mouse neocortex. CHL1 is unique among L1 recognition molecules in its graded expression, localizing to migratory precursors of pyramidal neurons in a high-caudal to low-rostral cortical gradient. In CHL1 null mutant mice, many deep layer pyramidal neurons were displaced to lower laminar locations in the visual and somatosensory cortex and developed apical dendrites with aberrant trajectories, while other neuronal populations showed more subtle malpositioning. Radial migration of cortical neurons in vivo and in organotypic brain slice cultures was strikingly reduced in the absence of CHL1. A mechanism in which CHL1 cooperates with β1 integrins to promote neuronal migration was suggested by the abil-

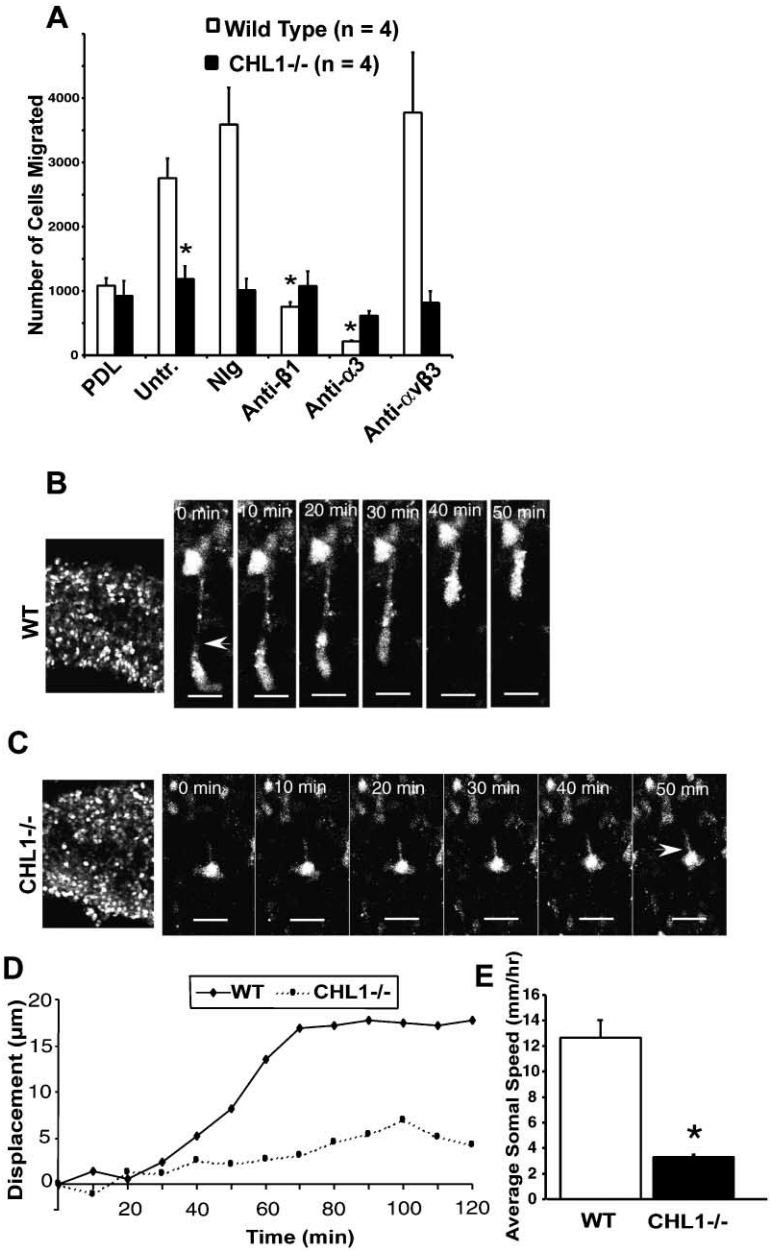


Figure 7. Radial Migration of Neurons in Acute Cortical Slices and Haptotactic Migration Assay

(A) Dissociated neurons from the caudal cortex of wild-type (n = 4) and CHL1-minus embryos (n = 4) at E14.5 were assayed for haptotactic migration to fibronectin in vitro for 22 hr. Cells were assayed for migration to poly-D-lysine (PDL) as control or fibronectin (Untr., untreated). Migration to fibronectin was measured in the presence of nonimmune IgG (NIg), function blocking antibodies against β1 integrin, α3 integrin, or αvβ3 (30 μg/ml). Samples were assayed in triplicate, and experiments were repeated twice. TuJ1 staining showed that 83% of wild-type cells were neurons; CHL1 staining showed that 50% of cells expressed CHL1. *Significant differences in means of wild-type versus CHL1-minus cells or normal Ig-treated versus β1- or α3 antibody-treated wild-type cells (Student's t test; $p < 0.05$). Scale bars, 100 μm.

(B–E) Time-lapse videoconfocal microscopy of wild-type (B) or CHL1-minus (C) neurons (E14.5) labeled with Oregon Green BAPTA-1 488 AM in slice cultures of caudal neocortex. Arrows, leading processes. (D) Radial somal displacement with time of a typical wild-type and CHL1-minus cell in the middle of the intermediate zone. (E) Average somal speed of labeled neurons measured over 2 hr for 53 wild-type neurons and 55 CHL1-minus neurons. *Significant difference (Student's t test, $p < 0.05$).

ity of CHL1 to potentiate integrin-dependent haptotactic migration of cortical neurons. Thus, selective expression of CHL1 in pyramidal precursors within posterior neocortical areas may modulate radial migration and enable cells to arrive at appropriate areal and laminar sites necessary for area-specific connectivity and, by extension, function.

### Mechanism of Cortical Migration Defects

Loss of CHL1 caused several disruptions in the development of the posterior neocortex: subpopulations of deep layer pyramidal neurons acquired inappropriately low laminar positions and exhibited misoriented, often inverted apical dendrites. The altered distribution of pyramidal cells in deeper regions of the visual and somatosensory cortex most likely reflected migration or positioning deficits rather than an increase in layer VI cells. Displaced neurons expressed the layer V-specific marker Er81, originated at the same time as deep layer pyramidal cells shown by BrdU labeling, and were identified as callosal and corticotectal projection neurons normally destined for layer V in the visual cortex by retrograde labeling with DiI. Furthermore, CHL1 was not expressed in the ventricular zone when cortical patterning was established (Rakic, 1988; Grove and Fukuchi-Shimogori, 2003), thus it is unlikely to control cell identity. The abnormal positioning of mutant neurons was not due to an altered distributions of Cajal-Retzius cells or radial glia, as the morphology and density of reelin-positive neurons and RC2-positive fibers were unaltered in CHL1 mutant mice. Altered laminar positioning and dendritic misorientation of deep layer mutant neurons was consistent with the preferential expression of CHL1 mRNA (Hillenbrand et al., 1999; Liu et al., 2000) and

CHL1 protein in subpopulations of pyramidal neurons of the developing posterior neocortex.

CHL1 mutant neurons destined for deep layers showed a pronounced reduction in radial speed in embryonic cortical slice cultures and haptotactic migration assays, suggesting impairment in migration. The accumulation of mutant neurons in the intermediate and ventricular/subventricular zones during development was in accord with this possibility. The slowly migrating CHL1-minus neurons in slices had atypically short, thin leading processes and rounded soma, unlike cells actively migrating in contact with radial glia. Such morphology was reminiscent of *weaver* neurons, which fail to bind appropriately to glial processes and are impaired for radial migration (Hatten et al., 1986). An adhesive role for CHL1 is indicated by its ability to promote HEK293 cell migration dependent on a cytoplasmic domain sequence that binds ankyrin (Buhusi et al., 2003), an actin cytoskeletal adaptor that stabilizes adhesive contacts.

CHL1 is unique among regulators of cortical lamination in preferentially modulating pyramidal cell distribution in posterior rather than anterior regions of the neocortex. The phenotype of the CHL1 knockout partly resembled $\alpha$3 integrin knockout embryos, in which the preplate is split and layer V/VI pyramidal cells are spread diffusely throughout and below the cortical plate (Anton et al., 1999). A major difference was that such defects were found only in posterior cortical areas of CHL1 mutants, whereas in $\alpha$3 mutants they were present throughout the cortex. The CHL1-minus cortex was also reminiscent of the doublecortin phenotype, in which there is preplate splitting and inappropriate laminar positioning with an accumulation of cells subcortically (Gleeson et al., 1999; Corbo et al., 2002; Bai et al., 2003). Abnormalities in the CHL1-minus cortex were distinct from reeler, scrambler, p35, cdk5, and LIS1 mutants, in which the preplate is not split and the laminar pattern is roughly inverted (Rakic and Caviness, 1995; Ohshima et al., 1996; Chae et al., 1997). Because CHL1 was enriched in deep layer neurons in the caudal cortex and was not expressed by all cells, its loss did not affect the positioning of all cortical neurons. Similiarly, mice deficient in molecules with important roles in migration, such as reelin and doublecortin, have some neurons with normal morphology and correct laminar position (Caviness, 1982; Pinto-Lord et al., 1982; Bai et al., 2003).

Although the CHL1 phenotype differs from reeler, scrambler, and others, it is fully consistent with general principles of cortical neuron migration. The reeler-like phenotype appears as a consequence of overattachment of early arriving neurons to radial glia, resulting in a backup of later-arriving cells (Caviness, 1982; Pinto-Lord et al., 1982). By contrast, the CHL1 phenotype may be a consequence of decreased adhesion of deep layer neurons to radial glia or, alternatively, defective somal translocation. If neurons deficient in CHL1 were less adherent to glial guides or impaired for translocation, they would not be expected to impede strongly the migration of later-arriving neurons. However, the altered location and dendritic development of deep layer neurons in the CHL1 mutant cortex could indirectly affect the migration and placement of other neuronal populations, as seen in the subtle malpositioning of upper and middle layer neurons and the delay of neurons destined for these layers. At present, however, we have no direct in vivo evidence to conclusively demonstrate that defective migration or adhesion accounts for the positioning defects observed in the CHL1 knockout.

Several lines of evidence do suggest that CHL1 has the potential to promote migration of cortical neurons through integrins. CHL1 potentiated integrin-dependent haptotactic migration to extracellular matrix proteins of embryonic cortical neurons, shown here and in HEK293 cells (Buhusi et al., 2003). CHL1 and $\beta$1 integrins associate directly or indirectly on the cell surface, share signaling intermediates (Src, PI3 kinase, ERK1/2) necessary for migration (Buhusi et al., 2003), and colocalize in subsets of migratory neurons. Potential crosstalk between integrins and reelin is suggested by the ability of the $\beta$ integrin cytoplasmic domain to interact with Dab-1, an intracellular adaptor involved in reelin signaling (Calderwood et al., 2003). Moreover, $\alpha$3 integrin promotes attachment of migrating cortical neurons to radial glia and must be downregulated for neuronal detachment in the later stage of migration dependent on Dab-1 (Sanada et al., 2004). Although $\beta$1 integrins have been shown to participate in radial migration of neurons in the developing chick tectum (Galileo and Linser, 1992; Zhang and Galileo, 1998; Stettler and Galileo, 2004), their involvement in cortical neuron migration is uncertain. Cortical lamination defects in a conditional $\beta$1 integrin knockout mouse were interpreted to result from detachment of radial glial endfeet from the meningeal basement membrane, displacing reelin-producing Cajal-Retzius cells, rather than a primary defect in migration (Graus-Porta et al., 2001). Such structural defects were not apparent in the CHL1-minus cortex. In the conditional knockout, loss of the $\beta$1 subunit may have disrupted the function of multiple $\alpha\beta$1 integrin subclasses, obscuring the role of a specific $\alpha$ integrin in migration. Indeed, knockouts of $\alpha$3 (Anton et al., 1999) or $\alpha$6 integrin genes (Georges-Labouesse et al., 1998) perturb the laminar organization of the cerebral cortex but do not display pial defects.

### Mechanism of Apical Dendrite Misorientation of Layer V Pyramidal Cells

Many displaced neurons in the CHL1-minus visual and somatosensory cortex exhibited an inverted polarity with apical dendrites oriented sideways or toward the ventricle. The size and projection features of the affected neurons in the CHL1 mutant visual cortex indicated that some were callosally projecting pyramidal neurons. Corticotectal neurons of layer V in the visual cortex were also displaced to lower cortical regions but did not show inverted polarity. Apical dendrites of callosally projecting neurons in deep layer V likely utilize specific regulatory mechanisms for orientation, as they are unique in undergoing active elimination to terminate in layer IV (Koester and O'Leary, 1992). One mechanism to explain the inverted apical dendrites of CHL1-minus pyramidal cells is that displacement of neurons to deeper regions may render them less responsive to factors from the upper cortical region, such as Sema3A, which attracts apical dendrites toward the pial surface (Polleux et al., 2000). Inversion of apical dendrites of cortical pyramidal cells is observed in Sema3A and *fyn*

mutant mice (Polleux et al., 2000; Sasaki et al., 2002), as well as in reeler (Caviness, 1976) and p35 mutants (Chae et al., 1997). Sema3A and *fyn* coordinately regulate apical dendrite orientation preferentially in layer V pyramidal cells (Sasaki et al., 2002). In this regard, it is interesting that L1 associates with Sema3A receptor neuropilin-1 through a sequence in the L1 IgI domain (Castellani et al., 2002) that is nearly identical in CHL1. Wavy, misoriented dendrites of pyramidal neurons have also been observed in the somatosensory and visual cortex of L1-minus mice (Demyanenko et al., 2001), suggesting that CHL1 and L1 may have overlapping functions in apical dendrite development in the posterior neocortex. Other L1 family members that are present in the developing cortex, such as NrCAM or neurofascin, which interacts with doublecortin (Kizhatil et al., 2002), might regulate similar events in the anterior cortex, where CHL1 expression is low.

## Experimental Procedures

### Mice

CHL1-minus mice on a C57Bl/6 × 129 genetic background (Montag-Sallaz et al., 2002) were intercrossed with Thy1/YFP (line H) transgenic mice (C57Bl/6 × non-Swiss albino), in which YFP is expressed postnatally from the Thy1 promoter in layer V pyramidal neurons throughout the cerebral cortex (Feng et al., 2000) to obtain homozygous CHL1 null mutants and wild-type controls from the same litters.

### Analysis of Cortical Neuron Location, Density, and Dendrite Orientation

For YFP analysis, brains of wild-type and CHL1 null littermates (P21–P28) were Vibratome sectioned at 200 μm in the sagittal plane. Cortical areas were identified by morphological criteria (Nauta and Feirtag, 1986) and comparison with atlas coordinates (Franklin and Paxinos, 1997). Nissl and Golgi staining were carried out as described (Demyanenko et al., 1999).

Scion Image software (NIH) was used to determine the migration index for each YFP-labeled neuron by calculating the distance of somata from the white matter relative to the cortical thickness. Migration index values were grouped into bins defined by the (1) 0–25th percentile, (2) 25th–75th percentile, and (3) 75th–100th percentile of migration index values for wild-type $YFP^+$ neurons in each cortical area. The percent of cells in each bin was determined for individual mice, and then means were compared by the Mann-Whitney rank sum test ($p < 0.05$). The percent of cells (graphed) represents a mean value obtained for individual mice and is not identical to the percentile, which represents a frequency based on the total number of cells.

For orientation of apical dendrites of YFP-labeled mice (P21–P28), Scion Image was used to defined a line from the center of the soma through the adjacent 100 μm of the dendrite. The angle (θ) made by this line relative to a line from the soma perpendicular to the pial surface was expressed in degrees (Figure 4B). Apical dendrites of wild-type $YFP^+$ neurons in all three neocortical regions were measured and found to have a mean angle of 0° ± 6° (1.5 standard deviations from the mean). Misoriented apical dendrites were thus defined as those with $|\theta| > 6°$. Inverted apical dendrites were defined as those with $|\theta| > 90°$. The percent of $YFP^+$ cells with misoriented or inverted apical dendrites was scored in each cortical region of individual mice (≥500 cells per genotype), and means were compared by the Mann-Whitney rank sum ($p < 0.05$).

Neuronal density was analyzed by scoring YFP-labeled neurons of large (≥18 μm) or small diameter (<18 μm) in wild-type ($n = 7$) and CHL1-minus ($n = 5$) mice. The mean neuronal number per $mm^2$ was calculated, and differences were compared by the Student's t test ($p < 0.05$). For each cortical region, 200 to 500 cells were scored per mouse. Spine densities of YFP-labeled pyramidal neurons were measured in confocal image projections (eight images, three mice, >900 spines per genotype) using Neurolucida software. Mean spine densities were compared by the Student's t test ($p < 0.05$).

### Antibodies and Immunofluorescence Staining

CHL1 rabbit polyclonal antibody 12146 was raised against recombinant CHL1 fused to the Fc portion of human IgG, and affinity purified as described (Chen et al., 1999). The antibody was specific for CHL1 shown by Western blotting at all stages in the mouse forebrain from E13-P15 and adult (Hillenbrand et al., 1999). Other antibodies used were rat monoclonal antibody MAB1997 against β1 subunit of VLA integrins (Chemicon), mouse monoclonal antibodies against MAP2 (Sigma), reelin (MAB5364; Chemicon), radial glial antigen RC2 (Developmental Studies Hybridoma Bank), TuJ1 recognizing neuronal class III β tubulin (Covance), and Er81 (Tom Jessell, Columbia University). Sections (12 μm) were incubated in blocking solution containing 2% bovine serum albumin (BSA), 20% normal goat serum and 0.2% Triton X-100 in PBS, and then in primary antibody overnight. Sections were incubated for 1 hr in fluorescein isothiocyanate (FITC) or tetramethyl rhodamine isothiocyanate (TRITC)-conjugated secondary antibodies (Jackson Immunoresearch; 1:200).

### Neuronal Birthdating with BrdU and DiI Labeling

For BrdU labeling of $YFP^+$ pyramidal cells in Figure 3, wild-type and CHL1-minus pregnant mice were injected intraperitoneally at E13.5 with BrdU (100 mg/kg body weight). At P21, brain sections were incubated with BrdU-specific monoclonal antibody (MAB3424 Chemicon; 1:100). For analysis of cortical positioning of neurons in other layers (Figure 6), BrdU injections (150 mg/kg) were done similarly at E11.5, E13.5, and E14.5, and brains were analyzed at P0. Cells were scored in distinct sectors of the cortex from multiple images, and means were compared for significance by the Student's t test ($p < 0.05$).

For retrograde labeling of corticotectal pyramidal neurons, a solution of DiI (10%; Molecular Probes) in dimethylformamide was injected into the superior colliculus of four wild-type and four CHL1-minus mice at P2 at the level of the stratum opticum, where corticotectal fibers terminate (Koester and O'Leary, 1992). After 48 hr, mice were perfused and brains were sectioned at 100 μm coronally. The migration index for each neuron was calculated as the distance of the soma from the white matter relative to the cortical thickness. Differences in mean migration index were compared by the Mann-Whitney rank sum test. For labeling callosally projecting neurons, DiI was injected at P5 into the visual cortex of three wild-type and four CHL1 mutant littermates and analyzed at P7. Labeling of neurons in the contralateral (callosal) and ipsilateral visual cortex was analyzed as for corticotectal neurons.

### Time-Lapse Confocal Videomicroscopy of Migrating Neurons in Acute Brain Slices

Cerebral hemispheres of embryos (E13.5) were sectioned coronally (150 μm) as described (Polleux et al., 2000), and caudal slices were incubated for 1 hr (37°C; 5% $CO_2$) in 12.5 μm Oregon Green BAPTA-1 488AM (Molecular Probes) in Neurobasal medium with 0.02% Cremophore, rinsed in medium, and transferred to glass bottom Microwell Dishes (MatTek Corporation) coated with extracellular gel matrix (Sigma). Slice cultures were incubated at 37°C in 5% $CO_2$ for 28 hr, and images were collected on a Zeiss LSM5 Pascal inverted confocal microscope. Image stacks were acquired every 10–20 min for 3–8 hr. Scion Image software was used to measure the position of the basal end of the soma on each image. Displacement of the soma was defined by the difference in location of this point in consecutive images. The somal speed was calculated as the displacement per unit time (μm/hr). Somal speeds were averaged, and standard errors were calculated for each population (wild-type and mutant). Statistically significant differences were determined by Student's t test (one-tailed; $p < 0.05$). In three separate experiments, 53 cells were analyzed from seven wild-type embryos, and 55 cells were analyzed from four CHL1 mutant embryos.

### Haptotactic Neuronal Migration Assay

Cortical neurons were dissociated nonenzymatically from the caudal half of the cortex by trituration from wild-type ($n = 4$) and CHL1-minus embryos ($n = 4$) at E14.5 as described (Anton et al., 1999;

Dulabon et al., 2000). Migration assays were performed in modified Boyden chambers with 8 μm pore filters (Transwells; Corning-Costar) as previously described (Buhusi et al., 2003). Fifty thousand live cells were plated per Transwell in serum-free Earle's balanced salt solution/16 mM glucose. Filters were pretreated with 0.1 mg/ml poly-D-lysine, then coated on the bottom with human fibronectin (Invitrogen, Gaithersburg, MD) (2.5 μg/filter). Migration of cells from top to bottom of filters was allowed to proceed for 22 hr. Some cells were preincubated with antibodies (30 μg/ml final) for 15 min at 4°C prior to assay. Antibodies included hamster anti-rat β1 integrin monoclonal antibody CD29 (Pharmingen Ha2/5; IgM), hamster IgM, mouse monoclonal antibody Ralph 3.1 against α3 integrin (Developmental Studies Hybridoma Bank), and anti-human αvβ3 integrin monoclonal antibody 1976Z (Chemicon; clone LM609). To score migration, cells were fixed in 4% paraformaldehyde and stained with hematoxylin. The percent of cells that migrated to the bottom of the filter was calculated as described (Buhusi et al., 2003). Experiments were done in duplicate or triplicate, and results were averaged. Means were compared by the Student's t test ($p < 0.05$; two-tailed). There was no loss of cell adhesion to the filters due to integrin antibodies, determined by comparing cells' recovery.

## Acknowledgments

This work was supported by NIH grants NS26620 and MH064056 (Silvio Conte Center for Neuroscience of Mental Disorders) and by NINDS Center grant P30NS045892 to the University of North Carolina Neuroscience Center for support of the Confocal Microscopy Facility. We thank Dr. Mona Buhusi for Western blotting; and Bentley Midkiff and Chris Ingersoll for expert technical assistance. Dr. Tom Jessell is gratefully acknowledged for providing Er81 antibody.

Received: November 20, 2003
Revised: April 15, 2004
Accepted: September 14, 2004
Published: October 27, 2004

## References

Angeloni, D., Lindor, N.M., Pack, S., Latif, F., Wei, M.H., and Lerman, M.I. (1999). CALL gene is haploinsufficient in a 3p- syndrome patient. Am. J. Med. Genet. *86*, 482–485.

Angevine, J.B., and Sidman, J.L. (1961). Autoradiographic study of cell migration during histogenesis of cerebral cortex in the mouse. Nature *192*, 766–768.

Anton, E.S., Kreidberg, J.A., and Rakic, P. (1999). Distinct functions of $\alpha_3$ and $\alpha_V$ integrin receptors in neuronal migration and laminar organization of the cerebral cortex. Neuron *22*, 277–289.

Bai, J., Ramos, R.L., Ackman, J.B., Thomas, A.M., Lee, R.V., and LoTurco, J.J. (2003). RNAi reveals doublecortin is required for radial migration in rat neocortex. Nat. Neurosci. *6*, 1277–1283.

Buhusi, M., Midkiff, B.R., Gates, A.M., Richter, M., Schachner, M., and Maness, P.F. (2003). Close homolog of L1 is an enhancer of integrin-mediated cell migration. J. Biol. Chem. *278*, 25024–25031.

Cahana, A., Escamez, T., Nowakowski, R.S., Hayes, N.L., Giacobini, M., von Holst, A., Shmueli, O., Sapir, T., McConnell, S.K., Wurst, W., et al. (2001). Targeted mutagenesis of Lis1 disrupts cortical development and LIS1 homodimerization. Proc. Natl. Acad. Sci. USA *98*, 6429–6434.

Calderwood, D.A., Fujioka, Y., de Pereda, J.M., Garcia-Alvarez, B., Nakamoto, T., Margolis, B., McGlade, C.J., Liddington, R.C., and Ginsberg, M.H. (2003). Integrin beta cytoplasmic domain interactions with phosphotyrosine-binding domains: a structural prototype for diversity in integrin signaling. Proc. Natl. Acad. Sci. USA *100*, 2272–2277.

Castellani, V., De Angelis, E., Kenwrick, S., and Rougon, G. (2002). Cis and trans interactions of L1 with neuropilin-1 control axonal responses to semaphorin 3A. EMBO J. *21*, 6348–6357.

Caviness, V.S., Jr. (1976). Patterns of cell and fiber distribution in the neocortex of the reeler mutant mouse. J. Comp. Neurol. *170*, 435–447.

Caviness, V.S., Jr. (1982). Neocortical histogenesis in normal and reeler mice: a developmental study based upon [3H]thymidine autoradiography. Brain Res. *256*, 293–302.

Chae, T., Kwon, Y.T., Bronson, R., Dikkes, P., Li, E., and Tsai, L.H. (1997). Mice lacking p35, a neuronal specific activator of Cdk5, display cortical lamination defects, seizures, and adult lethality. Neuron *18*, 29–42.

Chen, S., Mantei, N., Dong, L., and Schachner, M. (1999). Prevention of neuronal cell death by neural adhesion molecules L1 and CHL1. J. Neurobiol. *38*, 428–439.

Cohen, N.R., Taylor, J.S.H., Scott, L.B., Guillery, R.W., Soriano, P., and Furley, A.J.W. (1997). Errors in corticospinal axon guidance in mice lacking the neural cell adhesion molecule L1. Curr. Biol. *8*, 26–33.

Corbo, J.C., Deuel, T.A., Long, J.M., LaPorte, P., Tsai, E., Wynshaw-Boris, A., and Walsh, C.A. (2002). Doublecortin is required in mice for lamination of the hippocampus but not the neocortex. J. Neurosci. *22*, 7548–7557.

Dahme, M., Bartsch, U., Martini, R., Anliker, B., Schachner, M., and Mantei, N. (1997). Disruption of the mouse L1 gene leads to malformations of the nervous system. Nat. Genet. *17*, 346–349.

Demyanenko, G.P., and Maness, P.F. (2003). The L1 cell adhesion molecule is essential for topographic mapping of retinal axons. J. Neurosci. *23*, 530–538.

Demyanenko, G., Tsai, A., and Maness, P.F. (1999). Abnormalities in neuronal process extension, hippocampal development, and the ventricular system of L1 knockout mice. J. Neurosci. *19*, 4907–4920.

Demyanenko, G.P., Shibata, Y., and Maness, P.F. (2001). Altered distribution of dopaminergic neurons in the brain of L1 null mice. Brain Res. Dev. Brain Res. *126*, 21–30.

Dulabon, L., Olson, E.C., Taglienti, M.G., Eisenhuth, S., McGrath, B., Walsh, C.A., Kreidberg, J.A., and Anton, E.S. (2000). Reelin binds α3β1 integrin and inhibits neuronal migration. Neuron *27*, 33–44.

Feng, G., Mellor, R.H., Bernstein, M., Keller-Peck, C., Nguyen, Q.T., Wallace, M., Nerbonne, J.M., Lichtman, J.W., and Sanes, J.R. (2000). Imaging neuronal subsets in transgenic mice expressing multiple spectral variants of GFP. Neuron *28*, 41–51.

Franklin, K., and Paxinos, G. (1997). The Mouse Brain in Stereotaxic Coordinates (San Diego: Academic Press).

Frints, S.G.M., Marynen, P., Hartmann, D., Fryns, J.-P., Steyaert, J., Schachner, M., Rolf, B., Craessaerts, K., Snellinx, A., Hollanders, K., et al. (2003). *CALL* interrupted in a patient with non-specific mental retardation: gene dosage-dependent alteration of murine brain development and behavior. Hum. Mol. Genet. *12*, 1463–1474.

Galileo, D.S., and Linser, P.J. (1992). Immunomagnetic removal of neurons from developing chick optic tectum results in glial phenotypic instability. Glia *5*, 210–222.

Georges-Labouesse, E., Mark, M., Messaddeq, N., and Gansmuller, A. (1998). Essential role of alpha 6 integrins in cortical and retinal lamination. Curr. Biol. *8*, 983–986.

Gleeson, J.G., Lin, P.T., Flanagan, L.A., and Walsh, C.A. (1999). Doublecortin is a microtubule-associated protein and is expressed widely by migrating neurons. Neuron *23*, 257–271.

Graus-Porta, D., Blaess, S., Senften, M., Littlewood-Evans, A., Damsky, C., Huang, Z., Orban, P., Klein, R., Schittny, J.C., and Muller, U. (2001). β1-class integrins regulate the development of laminae and folia in the cerebral and cerebellar cortex. Neuron *31*, 367–379.

Grove, E.A., and Fukuchi-Shimogori, T. (2003). Generating the cerebral cortical area map. Annu. Rev. Neurosci. *26*, 355–380.

Hatten, M.E., Liem, R.K., and Mason, C.A. (1986). Weaver mouse cerebellar granule neurons fail to migrate on wild-type astroglial processes in vitro. J. Neurosci. *6*, 2676–2683.

Hevner, R.F., Daza, R.A., Rubenstein, J.L., Stunnenberg, H., Olavarria, J.F., and Englund, C. (2003). Beyond laminar fate: toward a molecular classification of cortical projection/pyramidal neurons. Dev. Neurosci. *25*, 139–151.

Hillenbrand, R., Molthagen, M., Montag, D., and Schachner, M. (1999). The close homologue of the neural adhesion molecule L1

(CHL1): patterns of expression and promotion of neurite outgrowth by heterophilic interactions. Eur. J. Neurosci. *11*, 813–826.

Holm, J., Hillenbrand, R., Steuber, V., Bartsch, U., Moos, M., Lubbert, H., Montag, D., and Schachner, M. (1996). Structural features of a close homologue of L1 (CHL1) in the mouse: a new member of the L1 family of neural recognition molecules. Eur. J. Neurosci. *8*, 1613–1629.

Jessell, T.M. (2000). Neuronal specification in the spinal cord: inductive signals and transcriptional codes. Nat. Rev. Genet. *1*, 20–29.

Kasper, E.M., Lubke, J., Larkman, A.U., and Blakemore, C. (1994). Pyramidal neurons in layer 5 of the rat visual cortex. III. Differential maturation of axon targeting, dendritic morphology, and electrophysiological properties. J. Comp. Neurol. *339*, 495–518.

Kenwrick, S., Watkins, A., and Angelis, E.D. (2000). Neural cell recognition molecule L1: relating biological complexity to human disease mutations. Hum. Mol. Genet. *9*, 879–886.

Kizhatil, K., Wu, Y.X., Sen, A., and Bennett, V. (2002). A new activity of doublecortin in recognition of the phospho-FIGQY tyrosine in the cytoplasmic domain of neurofascin. J. Neurosci. *22*, 7948–7958.

Koester, S.E., and O'Leary, D.D. (1992). Functional classes of cortical projection neurons develop dendritic distinctions by class-specific sculpting of an early common pattern. J. Neurosci. *12*, 1382–1393.

Komuro, H., and Rakic, P. (1992). Selective role of N-type calcium channels in neuronal migration. Science *257*, 806–809.

Kurumaji, A., Nomoto, H., Okano, T., and Toru, M. (2001). An association study between polymorphisms of L1CAM gene and schizophrenia in a Japanese sample. Am. J. Med. Genet. *105*, 99–104.

Liu, Q., Dwyer, N.D., and O'Leary, D.D. (2000). Differential expression of COUP-TFI, CHL1, and two novel genes in developing neocortex identified by differential display PCR. J. Neurosci. *20*, 7682–7690.

Marin, O., and Rubenstein, J.L. (2003). Cell migration in the forebrain. Annu. Rev. Neurosci. *26*, 441–483.

Miller, M.W. (1988). Maturation of rat visual cortex: IV. The generation, migration, morphogenesis, and connectivity of atypically oriented pyramidal neurons. J. Comp. Neurol. *274*, 387–405.

Montag-Sallaz, M., Schachner, M., and Montag, D. (2002). Misguided axonal projections, neural cell adhesion molecule 180 mRNA upregulation, and altered behavior in mice deficient for the close homolog of L1. Mol. Cell. Biol. *22*, 7967–7981.

Nadarajah, B., and Parnavelas, J.G. (2002). Modes of neuronal migration in the developing cerebral cortex. Nat. Rev. Neurosci. *3*, 423–432.

Nadarajah, B., Brunstrom, J.E., Grutzendler, J., Wong, R.O., and Pearlman, A.L. (2001). Two modes of radial migration in early development of the cerebral cortex. Nat. Neurosci. *4*, 143–150.

Nadarajah, B., Alifragis, P., Wong, R.O., and Parnavelas, J.G. (2003). Neuronal migration in the developing cerebral cortex: observations based on real-time imaging. Cereb. Cortex *13*, 607–611.

Nauta, W.J.H., and Feirtag, M. (1986). Fundamental Neuroanatomy (New York: Freeman).

Ohshima, T., Ward, J.M., Huh, C.G., Longenecker, G., Veeranna, Pant, H.C., Brady, R.O., Martin, L.J., and Kulkarni, A.B. (1996). Targeted disruption of the cyclin-dependent kinase 5 gene results in abnormal corticogenesis, neuronal pathology and perinatal death. Proc. Natl. Acad. Sci. USA *93*, 11173–11178.

Panicker, A.K., Buhusi, M., Thelen, K., and Maness, P.F. (2003). Cellular signalling mechanisms of neural cell adhesion molecules. Front. Biosci. *8*, D900–D911.

Pinto-Lord, M.C., Evrard, P., and Caviness, V.S., Jr. (1982). Obstructed neuronal migration along radial glial fibers in the neocortex of the reeler mouse: a Golgi-EM analysis. Brain Res. *256*, 379–393.

Polleux, F., Morrow, T., and Ghosh, A. (2000). Semaphorin 3A is a chemoattractant for cortical apical dendrites. Nature *404*, 567–573.

Pratte, M., Rougon, G., Schachner, M., and Jamon, M. (2003). Mice deficient for the close homologue of the neural adhesion cell L1 (CHL1) display alterations in emotional reactivity and motor coordination. Behav. Brain Res. *147*, 31–39.

Rakic, P. (1988). Specification of cerebral cortical areas. Science *241*, 170–176.

Rakic, P., and Caviness, V.S., Jr. (1995). Cortical development: view from neurological mutants two decades later. Neuron *14*, 1101–1104.

Rice, D.S., Sheldon, M., D'Arcangelo, G., Nakajima, K., Goldowitz, D., and Curran, T. (1998). Disabled-1 acts downstream of Reelin in a signaling pathway that controls laminar organization in the mammalian brain. Development *125*, 3719–3729.

Sakurai, K., Migita, O., Toru, M., and Arinami, T. (2002). An association between a missense polymorphism in the close homologue of L1 (CHL1, CALL) gene and schizophrenia. Mol. Psychiatry *7*, 412–415.

Sanada, K., Gupta, A., and Tsai, L.-H. (2004). Disabled-1-regulated adhesion of migrating neurons to radial glial fiber contributes to neuronal positioning during early corticogenesis. Neuron *42*, 197–211.

Sasaki, Y., Cheng, C., Uchida, Y., Nakajima, O., Ohshima, T., Yagi, T., Taniguchi, M., Nakayama, T., Kishida, R., Kudo, Y., et al. (2002). Fyn and Cdk5 mediate semaphorin-3A signaling, which is involved in regulation of dendrite orientation in cerebral cortex. Neuron *35*, 907–920.

Sheppard, A.M., and Pearlman, A.L. (1997). Abnormal reorganization of preplate neurons and their associated extracellular matrix: an early manifestation of altered neocortical development in the reeler mutant mouse. J. Comp. Neurol. *378*, 173–179.

Sheppard, A.M., Hamilton, S.K., and Pearlman, A.L. (1991). Changes in the distribution of extracellular matrix components accompany early morphogenetic events of mammalian cortical development. J. Neurosci. *11*, 3928–3942.

Stettler, E.M., and Galileo, D.S. (2004). Radial glia produce and align the ligand fibronectin during neuronal migration in the developing chick brain. J. Comp. Neurol. *468*, 441–451.

Takahashi, T., Nowakowski, R.S., and Caviness, V.S., Jr. (1996). Interkinetic and migratory behavior of a cohort of neocortical neurons arising in the early embryonic murine cerebral wall. J. Neurosci. *16*, 5762–5776.

Thelen, K., Kedar, V., Panicker, A.K., Schmid, R.S., Midkiff, B.R., and Maness, P.F. (2002). The neural cell adhesion molecule L1 potentiates integrin-dependent cell migration to extracellular matrix proteins. J. Neurosci. *22*, 4918–4931.

Zhang, Z., and Galileo, D.S. (1998). Retroviral transfer of antisense integrin $\alpha 6$ or $\alpha 8$ sequences results in laminar redistribution or clonal cell death in developing brain. J. Neurosci. *18*, 6928–6938.